Allometry and advancing age significantly structure craniofacial variation in adult female baboons

Jessica Joganic, Yann Heuzé

Allometry and advancing age significantly structure craniofacial variation in adult female baboons☆

Jessica L Joganic[a,b,*], Yann Heuzé[c]

[a]*Univ. Bordeaux, CNRS, MCC, PACEA, UMR5199, 33615 Pessac Cedex, France*
[b]*Dept. Anthropology, Washington University in St. Louis, One Brookings Drive, Campus Box 1114, St. Louis, Missouri 63130-4899*
[c]*CNRS, Univ. Bordeaux, MCC, PACEA, UMR5199, 33615 Pessac Cedex, France*

Abstract

Primate craniofacial growth is traditionally assumed to cease upon maturation, or at least be negligible, while bony remodeling is typically associated with advanced adult age and, in particular, tooth loss. Therefore, size and shape of the craniofacial skeleton (CFS) of young and middle-aged adults should be stable. However, research on both modern and historic human samples suggests that portions of the CFS exhibit age-related changes in mature individuals, both related to and independent of tooth loss. These results demonstrate that the age-category "adult" is heterogeneous, containing individuals demonstrating post-maturational age-related variation, but the topic remains understudied outside of humans and in the cranial vault and base. Our research quantifies variation in a sample of captive adult female baboons (N = 97) in an effort to understand how advancing age alters the mature CFS. Craniometric landmarks and sliding semilandmarks were collected from CT scans of adult baboons aged 7–32 years old. To determine if craniofacial morphology is sensitive to aging mechanisms and if any such effects are differentially distributed throughout the cranium, geometric morphometric techniques were employed to compare the shapes of various cranial regions among individuals of increasing age. Unexpectedly, the biggest form differences were observed between young and middle-aged adults, rather than between adults with full dentitions and those with some degree of tooth loss. Shape variation was greatest in masticatory and nuchal musculature attachment areas. Our results indicate that the CFS changes form during adulthood in baboons, raising interesting questions about the molecular and biological mechanisms governing these changes.

Keywords: *Papio*, geometric morphometrics, allometry, post-maturational aging

1. Introduction

Bone growth (change in size over time) and development (change in shape over time) are governed by the molecular and hormonal signalling cascades that regulate and coordinate os-

☆*Running title:* **Craniofacial aging in adult female baboons**

*Corresponding author
Email address: jjoganic@wustl.edu (Jessica L Joganic)

teoblastic secretion and osteoclastic resorption of the composite protein-and-mineral matrix forming the molecular structure of bone (Enlow, 1975). Consequently, skeletal maturation is a complex interplay of epigenetic, hormonal, biochemical, and mechanical factors (Biewener and Bertram, 1993). Post-natal bone growth occurs via both periosteal expansion (appositional growth) and sutural/synchondroseal/epiphyseal displacement (longitudinal growth). However, modification to the size and shape of the mature skeleton proceeds differently (e.g., Frost, 1969; Currey, 1984), as the growth sites have ossified and longitudinal growth is no longer possible. Additionally, cortical drift (remodeling) can modify the shape of pre-existing bone by altering the relative rates of endosteal resorption and periosteal deposition (Boskey and Coleman, 2010). In this way, bone tissue can adapt to the environmental demands of an organism, helping to ensure that an individual's skeleton is biomechanically optimized over the course of their lifetime. However, the mechanotransductive properties (the ability of cells to sense, process, and respond to mechanical stimuli) of bone cells are altered with increasing age (Wu et al., 2011), potentially recurrently modifying the remodeling process throughout adulthood.

Fusion of the spheno-occipital synchondrosis and eruption of the third molars are traditionally accepted as the craniofacial features in humans and non-human primates that define an individual as being an "adult" (e.g., Bramblett, 1969; Falk et al., 1989; Wang et al., 2006; Zihlman et al., 2007; Poe, 2011; Franklin and Flavel, 2014; Balolia, 2015). As it is assumed that processes of skeletal maturation largely function the same in the craniofacial skeleton (CFS) and long bones (e.g., Litsas, 2015; Wei et al., 2016), and because the limbs cease growing when individuals reach adulthood, craniofacial growth in adult individuals is traditionally considered to be nonexistent or negligible (Shea, 1998; Bastir et al., 2006; Matros et al., 2009, see also the discussion by G. Northcroft accompanying Hellman, 1927). However, an accumulation of research in the orthodontic, aesthetic plastic surgery, and forensic literature suggests this assumption is invalid (see reviews by Israel, 1973b; Behrents, 1985;

Mendelson and Wong, 2012; Albert et al., 2007).

There are four main deficits in the literature regarding the study of post-maturational age-related effects in the CFS. First, the vast majority of such research is conducted in humans (although, see Hens, 2005; Wang et al., 2007; Balolia et al., 2013; Minh et al., 2015), so it is difficult to determine what effects dietary shifts and the reorganization of the hominin cranium may have had on any general mammalian patterns of post-maturational craniofacial aging. Second, most research considers only the facial skeleton. There are only a few examples in the clinical literature that include the cranial base or vault (e.g. Zuckerman, 1955; Bondevik, 1995). Third, research conducted on the subject of aging in the adult CFS deals almost exclusively in linear dimensions and angular measurements. Consequently, a considerable amount of data exists that demonstrates size increase of the CFS in adults, but far less is known about its development and any allometric (co-variation in shape and size) trends. A few of the more recent studies use geometric morphometric methods, which are often preferred for studying shape variation as they preserve the geometry among landmarks (e.g., Bastir et al., 2006; Williams and Slice, 2010), but much more research on post-maturational shape variation is needed. Fourth, very few studies consider the effects of bone resorption independent of tooth loss (although, see Pessa et al., 1998; Mendelson et al., 2007) because, in general, the majority of research on growth trends in adult crania suggests that "craniofacial bony aging, contrary to popular belief, is one of expansion and not of atrophy" (Bartlett et al., 1992).

1.1. CFS aging effects in adult humans

Considerable research on age-related growth in the human head has been conducted, starting in 1858 with Sir George Murray Humphry who recognized that bones of the cranial vault increase in thickness with age (cited in Bartlett et al., 1992). Additional early work demonstrated that cranial growth continues throughout the life of an individual (Todd, 1924; Hrdlička, 1925; Hellman, 1927; Israel, 1968) and, in the facial skeleton at least, increases in

rate later in life (Hooton and Dupertuis, 1951; Lasker, 1953). A study by Israel (1973a) indicated an overall size increase on the order of 5–7%, although a greater expansion is observed in cranial vault thickness than in global width or length (Israel, 1977). These patterns are sexually dimorphic (e.g., Formby et al., 1994; Williams and Slice, 2010) and observable in both modern and historic populations (e.g., Herzberg and Holic, 1943; Ruff, 1980; Bartlett et al., 1992).

Across a sample of five human populations that differ in geographic region of origin and chronological age, Guagliardo (1982) discovered a number of common post-maturational aging patterns in CFS shape. These included a flattening of the frontal bone profile, increased facial protrusion, widening of various interorbital dimensions, subnasal retraction in relation to the zygomatic arches, and a general increase in the size of both the orbits and the mastoid region. He attributed these changes to a lifetime of strain in response to the stresses of bite forces and exertion of the masticatory muscles.

The majority of research on post-maturational aging in the CFS, especially as it relates to facial rejuvenation surgery and dental orthotics for edentulous individuals, is conducted by clinicians in contemporary humans (see reviews by Mendelson and Wong, 2012; Wulc et al., 2012) or in non-human primates, particularly those experimentally manipulated for orthodontic research (e.g., Jaul et al., 1980; Minh et al., 2015). According to a review of the aging literature by Albert et al. (2007), the following changes have been observed in various human skeletal and radiographic samples: (1) horizontal dimensions of the face increase in size, particularly the distance between the cheekbones (i.e., bizygomatic breath); (2) anterior facial height (chin to nasal bridge) increases, primarily in the lower $\frac{4}{5}$ of the face; (3) continued eruption of the teeth increases facial height, while temporomandibular joint (TMJ) arthritis and dental attrition can decrease it; (4) the maxilla is often displaced posteriorly (although, see Levine et al., 2003); (5) absolute cranial bone thickness is greater in females and increases until 65 years old; and (6) variation in cranial bones thickness is

greater in males and remains constant over time, yet absolute thickness steadily decreases with age. The authors note that these changes are small (on the order of 1.1–1.6 mm) but noticeable.

1.2. The influence of tooth loss

Both tooth loss and subsequent bone resorption are acknowledged to alter the size and shape of the anterior midface, palate, and mandible (e.g., Tallgren, 1974; Jaul et al., 1980; Xie et al., 1997; Sutton et al., 2004; Dechow et al., 2010). However, it is not until individuals reach an advanced age that the effects of such remodeling on the CFS are usually deemed a potential source of intraspecific variation. Consequently, age is often incorporated as a covariate in regression models or landmarks located in areas expected to be affected by resorption, such as alveolar bone, are omitted from further analysis. Alternatively, individuals demonstrating CFS remodeling are often avoided, if possible. Depending on the organism being studied, this practice can result in a sample comprised of a range of individuals who are somatically mature but that do not yet demonstrate macroscopic signs of aging. Such a sample of wildly varying ages has the potential to bias any resulting inferences that are made.

Additionally, the potential effects of tooth loss and remodeling of alveolar bone on portions of the CFS not directly associated with the oral cavity are rarely considered. There is debate as to whether the same patterns of craniofacial variation are observed in elderly individuals who retain all their teeth (e.g., Herzberg and Holic, 1943; Pessa et al., 1998). Due to the changing material properties of bone as it ages (Colman et al., 1999; Boskey and Coleman, 2010), one might expect similar aging effects in both elderly individuals who retain all their teeth and their partially edentulous conspecifics. Alternatively, as tooth loss significantly alters the material properties of bone (Dechow et al., 2010), it may be entirely possible that the difference in craniofacial morphology is so drastic as to be easily accounted for when examining morphological variation in aged individuals. It is also unclear whether

other factors, such as regional muscle atrophy, may affect the aging cranium in both humans and other mammals.

1.3. CFS aging effects in other animals

It is possible that these recognized changes in the human adult CFS are related to the fact that the introduction of cooked and less mechanically demanding foodstuffs into our diets has caused facial shortening and the resultant malocclusion issues that plague modern humans (Begg, 1954; Larsen, 1995; Lieberman et al., 2004). In addition, the conformation of the CFS has been drastically reorganized in humans to accommodate our greatly encephalized brains (Lieberman, 2008). Therefore, it is both interesting and informative to look at patterns of CFS post-maturational change in other animals to ascertain whether the trends in size and shape change published in the literature thus far are also unique to humans. If they are, we may need to revisit our use of non-human model organisms in craniofacial research.

Outside of humans, the effects of normal post-maturational aging on the CFS, and in particular the portions of the skull not immediately involved in the oral cavity, are neither well-studied nor often considered a potential source of variation in biological, evolutionary, or anthropological research. The use of non-human primates and other mammals, particularly macaques and rabbits, to explore the response of the CFS to orthodontic and endodontic treatments is popular (e.g., Legan and Nanda, 1978; Jaul et al., 1980; Ramfjord and Blankenship, 1981; Rafferty et al., 2012). Consequently, a considerable amount of evidence has been amassed that maxillary growth results from surgical intervention, even in adults, but less research has been done to uncover the natural patterns of CFS change in post-maturational individuals.

Although ontogenetic growth and development of the primate CFS has been the subject of considerable research (e.g., Collard and O'Higgins, 2001; Mitteroecker et al., 2004a,b, 2005; Leigh, 2006; Singleton, 2012), very few studies extend the observational period into adulthood. However, there are three recent studies that provide evidence for post-maturational

changes to the CFS in non-human primates. Minh et al. (2015) present data on captive adult Japanese macaques indicating that cranial length increases more than breadth, the magnitude of post-maturational changes are greater in macaques than in humans, and most changes are observed in male, rather than female, macaques. In contrast, Wang et al. (2007) demonstrated that CFS development of rhesus macaques is characterized by faster male growth rates during adolescence (2–8 years) and an extended female growth period (8–15 years). Finally, Balolia et al. (2013) show that hominoid facial dimensions increase in size after the attainment of sexual maturity in male and female orangutans and gorillas, female gibbons, and likely female chimpanzees, although they lacked the power to definitively conclude the trend is visible in *Pan* as well. In all cases, because the increases were more pronounced between younger adult age categories, the authors conclude that ontogentic trajectories are extended past the age of adolescence and that this may be a feature of female growth and development with deep evolutionary roots.

1.4. Research questions

To address the stated deficits in the aging literature and extend what little work has been done to an additional primate species, we evaluate multivariate age-related changes in craniofacial morphology by quantifying normal variation in the aging CFS from a large number of known-aged and diet-controlled adult female baboons. A major benefit of using this sample is that all individuals were maintained in a similar and constant environment during the entirety of their lives, thereby greatly reducing the effects of dietary and activity pattern variability. Sexual size and shape dimorphism in the CFS is extreme in baboons (e.g., Leigh and Cheverud, 1991; O'Higgins and Collard, 2002; Singleton, 2002). As the focus of this paper is on age-related variation, we elected to study only one sex and chose females because the presence of a C-P3 honing complex and the variable sagittal crest size in males unnecessarily introduces additional sources of variation. Allometry, or shape variation that is a consequence of differences in the size of individuals, is also an important source of intraspe-

cific variation, particularly in baboons (e.g., Frost et al., 2003; Porto et al., 2009; Joganic et al., 2018). Thus, it will be especially important to determine whether any demonstrated age-related shape variation in the baboon CFS can actually be attributed to allometry.

Using geometric morphometric techniques and multivariate statistics, we address three specific questions. First, are there measurable differences in the patterns of craniofacial variation as individuals age? Second, what role does allometry play in the manifestation of any age-related shape variation? And third, if patterns of CFS size and shape variation are observable across adulthood, are different regions of the skull affected in the same manner? Based on previous research (e.g., Zuckerman, 1955; Bartlett et al., 1992; Bondevik, 1995), some regions are expected to demonstrate age-related changes (e.g., the midface) while others are expected to remain invariant across age categories (e.g., the basicranium). These analyses will tell us if craniofacial morphology is sensitive to aging mechanisms and if any such effect is differentially distributed throughout the skull.

2. Methodology

2.1. Baboon sample

A large colony of baboons (*Papio* ssp.) is maintained by the Southwest National Primate Research Center in San Antonio, Texas. The colony was founded with wild-caught animals from a region of southwestern Kenya overlapping Tsavo East National Park (Maples et al., 1967). Careful breeding to maintain as much of the original genetic diversity as possible has been practiced and has resulted in a seven-generation pedigree preserving 12 founding sire lines. The skulls from a portion (N = 985) of the pedigreed population were curated and CT scanned (0.6–0.75 mm resolution) at Washington University in St Louis and are now housed at Loyola University Chicago (LUC) under the care of Dr. James Cheverud (see Joganic et al., 2018 for more details).

There are 653 adult females in the LUC baboon collection. Individuals are considered

adult if they possess a fused spheno-occipital synchondrosis and fully occluded M3's. The average age of this total sample of adult females is 19.83 ± 5.5 years (range: 6.23–33.70). Four groups were created: individuals in the bottom age quartile (Young Adult, YA), within 0.5 standard deviations of the mean age (Adult, AD), in the top age quartile with full dentitions (Elderly, ER), and in the top age quartile with some degree of maxillary tooth loss (Tooth Loss, TL). A subset of 25 individuals was randomly selected from each group, except in the case of the TL category, for which only 22 individuals could be identified who were missing at least one maxillary tooth and had complete crania (N = 97; Table 1, Supp. Table S1). The modal number of maxillary teeth missing in TL individuals is 1 (mean: 2.14, range: 1-5), while all individuals in the three other age categories have full maxillary dentitions.

[Table 1 about here.]

2.2. Landmarking

Our three research questions deal specifically with the effect of post-maturational aging on differences in CFS shape. Shape is the portion of an object's geometry that is independent of overall size, position in space, or relative orientation (Mitteroecker and Gunz, 2009). Linear distances calculated between landmark pairs are particularly good at capturing variation in size, both relative and overall, but are less useful for quantifying shape differences. Traditional geometric morphometrics utilizes configurations of homologous landmarks strategically placed on an object that are then compared to a reference configuration (Bookstein, 1996). This method of studying shape can be problematic as the researcher is limited to using easily-identifiable and biologically homologous traits, such as the intersection between two bones or the point of the chin. Bones of the cranial vault are relatively featureless, making the identification and placement of anatomical landmarks difficult. Semilandmarks (or sliding landmarks, SL), on the other hand, are ideal for studying smooth curves and surfaces.

For our purposes here, semilandmarks allow us to capture changes in concavity/convexity (e.g., maxillary retrusion and nasal protrusion can alter the relationship between the midface and the upper and lower face as individuals age; Mendelson et al., 2007) and in profile (different CFS regions have been shown to become more or less prominent with age, properties best studied in profile; Bartlett et al., 1992) of regions displaying a very small number of traditional landmarks.

We examined three anatomical regions of the CFS in our subsample of 97 female baboons: facial skeleton (including the orbits, zygomatic arches, and palate), cranial vault, and cranial base (Fig. 1). These were selected because they are the traditionally recognized modules of the cranium relating to functional and developmental specializations (Cheverud, 1982, 1995).

[Figure 1 about here.]

We used Avizo Standard v 8.1.1 (FEI Visualization Sciences Group) to visualize the CT images, reconstruct the skulls, identify 43 craniometric landmarks (Table 2), and make surface mesh files. Viewbox v 4.0.1.7 (dHAL software, Athens, Greece) was then used to measure curve and surface SL on these surface meshes by applying a thin plate spline deformation to a template landmark configuration (Gunz and Mitteroecker, 2013). This protocol has been described elsewhere (Heuzé et al., 2010) but, briefly, after being manually placed on a single individual to create a template, the reference landmark configuration is fit to other individuals according to an algorithm that minimizes the bending energy while sliding SL along their identified curves and surfaces.

[Table 2 about here.]

The template we constructed consisted of four curves and six surfaces. An open curve of 15 SL was fit to each orbital margin (supraorbital notch to a point on the medial orbital

margin at the level of nasion) and an open curve of 9 SL to each zygomatic arch (frontozygomatic foramen to superior zygotemporal suture) for a total of 48 curve SL. The 210 surface SL were divided among six patches located on the left and right face (30 SL each), forehead (30 SL), left and right vault (40 SL each), and occiput (40 SL). Facial patches covered the entirety of the anterior surfaces of the malars, nasals, maxillae, and premaxillae, except for the alveoli, pyriform aperture, orbital margins, and zygomatic temporal processes. The forehead patch was defined as the triangular area bordered by the superior orbital margin and superior temporal lines. Vault patches covered the surface of the neurocranium from the superior temporal line/crest to the nuchal crest. The occiput consisted of the trapezoidal region bordered by the nuchal crest, posterior margin of the foramen magnum, and the mastoid processes. To construct the template, each patch was identified on the surface mesh by highlighting the desired area using the paintbrush tool in Viewbox. Then, we used the functions `Distribute on mesh (random)` followed by `Diffuse points uniformly` to associate the SLs with their corresponding patches. Our protocol resulted in a template with a total of 301 landmarks and SL to be identified for each individual (see Fig. 1 and Table 2).

2.3. Statistical shape analysis

A Generalized Procrustes superimposition (Rohlf and Slice, 1990; Goodall, 1991) to remove the aspects of variation in which we are not interested (differences in overall size, relative orientation, and spatial position) results in shape data in the form of Procrustes shape coordinates (PSCs). To address the research questions, we performed a multivariate multiple regression ("primary shape regression") of the PSCs on centroid size (CS), chronological age (hereafter referred to as age), and number of teeth missing (Mitteroecker and Gunz, 2009). This analysis tests the null hypothesis that post-maturational CFS variation is not structured by cranial size, age, or tooth loss. A Type II MANOVA is then used to test whether each explanatory variable is significant after controlling for the others. Centroid size is a method

of approximating size by calculating the square root of the sum of the squared distances of a set of landmarks from their centroid, the centroid being the mean x,y,z of all coordinates across all landmarks (Klingenberg, 2016). This is important for determining whether CFS shape changes with age simply because adult individuals increase in size with age or because there are shape differences between younger and older adults that cannot be accounted for by size differences among the age categories. All analyses were performed in MorphoJ v 1.06d (Klingenberg, 2011) and RStudio using the *Morpho* v 2.6 (Schlager, 2017) and *geomorph* v 3.0.6 (Adams et al., 2018) packages.

To visualize the shape changes related to CS and age, heat maps were created by deforming the template surface mesh in Avizo (Heuzé et al., 2014). The template surface mesh was shifted into shape space by morphing it according to the coordinates of the Procrustes mean shape. The PSCs for an individual at the extreme small end of the multivariate regression of shape on CS were calculated from the regression equation (small PSCs) and the same was done for an individual on the extreme large end (large PSCs). Then, "small" and "large" surface meshes were created by morphing the Procrustes mean shape mesh by the small and large PSCs, respectively. Finally, a displacement field was created using the `Vertex Difference` function, which calculates vectors between the vertices of each triangle in the reference surface mesh and the corresponding vertices of the homologous triangle in the target surface mesh. The reference surface mesh was then colored according to the magnitude of the vectors, allowing the viewer to discern "hot spots" of change between the two surface meshes. The small surface mesh was selected as the reference and the large as the target, so the visualized displacement field demonstrates regions that experience major change as individuals increase in size. The same procedure was done for age with the reference surface representing a younger adult and the target an older one, thus demonstrating regions where age-related differences are concentrated. It is important to emphasize that the differences represented by the heat maps are not those between an actual young/small individual and an

old/large one, but represent the extremes of the shape variation vectors that are statistically correlated with age and size, respectively.

1. Growth and allometry. We addressed the question of post-maturational growth in female baboons in three ways. First, we performed an ordinary least squares (OLS) regression of CS on age to test the null hypothesis that size of the CFS is static once sexual maturity is achieved. Second, we performed a one-way ANOVA to determine which, if any, of the age-groups differed in CS. Third, we looked at the effect of size on the shape of the cranium as a whole (i.e., allometry) by examining the coefficient of the CS term in the primary shape regression.

2. Age-related shape variation. We examined both age effects and the effect of tooth loss on global cranial shape variation. To identify whether shape differences exist among age groups, we calculated the consensus configuration (or mean shape) specific to each group. For example, a YA mean shape was computed as the coordinate-wise average of the PSCs of the individuals in the youngest age category. These mean shapes were compared between the different age groups using the metric of Procrustes distance, the square root of the sum of the squared Euclidean distances between each landmark in a configuration and its homologous landmark in the sample mean configuration. To test for significant group differentiation, a Procrustes ANOVA was performed, which models the Procrustes distances among specimens, rather than explained covariance among variables (Goodall, 1991). Then, to determine how much of the global variation in CFS shape can be explained adequately by age, we examined the beta coefficient of the age term from the primary shape regression.

Finally, we tested the null hypothesis that tooth loss has no observable effect on the CFS in two ways. We compared the Procrustes distances of the ER and TL groups using a permutation test to determine statistical significance. This type of analysis considers tooth loss as a binary variable, as ER individuals have all maxillary teeth present and TL individuals have lost at least one maxillary tooth. To perform a more nuanced analysis of the

effect of tooth loss on CFS shape, we also coded TL individuals by the number of maxillary teeth missing and performed a multivariate multiple regression ("dental shape regression") using the PSCs as dependent variables and CS, age, and number of teeth lost as independent variables.

3. Region-specific aging effects. PSCs were calculated separately for each of the three craniofacial regions by performing three distinct Generalized Procrustes superimpositions. The resulting alignments are referred to as the vault PSCs (n = 110 landmarks), base PSCs (n = 50), and face PSCs (n = 141). A multivariate multiple regression was performed for each of the regional PSCs ("[*region*] shape regression"). All three regressions contained the same three explanatory variables as the primary shape regression (CS, age, number of teeth lost). Procrustes ANOVA was used to test for significant age-group differentiation in the morpho space of each craniofacial region.

3. Results

3.1. The effects of age on size

First, we assessed the impact that aging has on cranial size. There is a 1.8% increase in CS between the YA and AD groups, a 2.8% increase between the YA and ER groups, and a 2.4% increase between the YA and TL groups (Fig. 2). If the three older groups are combined, the pooled mean CS is 2.4% larger than the YA mean CS, and this difference is statistically significant (Welch's t-test: $\bar{X}_{YA} = 927.5, \bar{X}_{pooled} = 949.9, t = -3.76, P = 0.0004$). Age explains 14.5% of the variance in CS (OLS: $t = 4.2, P < 0.001$; Fig. 3).

[Figure 2 about here.]

[Figure 3 about here.]

3.2. The effects of size on shape

In the primary shape regression, the CS term is highly significant ($F = 4.37, P = 0.001$) and accounts for 4.3% of the variance in the PSCs (Table 3; Supp. Fig. S1). Larger individuals have a longer snout, a more narrow midface and shorter posterior facial height, smaller and more ellipsoid orbits, and a neurocranium that is more ovoid in shape. Smaller individuals are more brachycephalic and have large, round orbits and more flaring malars (Supp. Videos 1–4).

[Table 3 about here.]

3.3. The effects of age on shape

To determine whether the four groups differed in CFS shape, Procrustes distances between the PSCs of the groups were calculated (Table 4). The YA group is significantly distinct from the other three in the morphospace, which cluster together (Supp. Fig. S2). This result is confirmed with a Procrustes ANOVA. When comparing all four groups, the F-statistic is marginally significant ($F = 1.48, P = 0.06$), but when pooling the AD, ER, and TL groups, the shape of the YA group is significantly different from that of the older individuals ($F = 3.02, P = 0.006$).

[Table 4 about here.]

In the primary shape regression, age accounts for a modest but significant 2.7% ($P = 0.005$) of the sample variation (see Table 4. Young individuals are characterized by globular neurocrania, wide midfaces, and a more flexed cranial base, while elderly individuals have a more elongated and widened snout, prominent inion, concave nasal bridge with a retruded midface, and a flattened nuchal plane (Supp. Videos 5–8). Although the size and age effects share some commonalities (e.g., both young and small individuals have shorter snouts than

older and larger individuals; Fig. 4), there are some important distinguishing features. Overall, the allometric trend gives a sense of a small cranium being stretched in the sagittal plane, primarily in the facial skeleton, to produce a large one. Additionally, the premaxillary dentition is displaced inferiorly, resulting in an increasing degree of klinorhynchy as crania increase in size. In contrast, the age trend is best characterized as an anterior and superior movement of the anterior face in the sagittal plane and a recession of the midface with a concomittant protrusion of the midline upper face.

[Figure 4 about here.]

Two methods were applied to determine the effect of tooth loss as quantified in either a binary or an ordinal manner. A Procrustes ANOVA performed only on the ER and TL groups indicates the two are not significantly different ($F = 0.64, P = 0.80$). This suggests that, in a global sense, whether an individual has lost any teeth has no marked effect on shape of the CFS. The second method, the dental shape regression, provides a more nuanced examination by testing the effect of the *number* of teeth lost. Although 9.0% of CFS shape variation within the TL category is accounted for by the number of teeth missing, after correcting for multiple comparisons (within-model Bonferroni; Mundfrom et al. 2006) this effect is rendered non-significant ($\alpha = \frac{0.05}{3} = 0.017, P = 0.038$; see Table 3). As statistical power may be limited by the small number of individuals within each TL sub-category (range: 1–10, mean: 4.6), future research may yet provide stronger evidence for a link between tooth loss and facial shape. Our results suggest that individuals with a greater number of teeth missing tend to have larger positive regression scores for the dental shape regression (Supp. Fig. S3), which are associated with a more arched palate, a superior and posterior shift of all alveolar landmarks, a more horizontal premaxillary profile, and a slightly wider breadth across the midface and orbits.

3.4. Size and age effects by region

According to the region-specific Procrustes ANOVA, there were no group differences in shape of the vault ($F = 0.89, P = 0.62$) or base ($F = 1.16, P = 0.23$), but the face PSCs differed significantly among the age categories ($F = 2.10, P = 0.008$). Using Procrustes distance as a metric, YA individuals are separate from all other groups in the facial morphospace (Supp. Table S2).

Centroid size explains 2.8% ($P = 0.007$) of the total variation in vault PSCs (see Table 3), with a contrast between dolicocephalic large individuals and brachycephalic small ones. Age accounts for a marginally insignificant 1.8% ($P = 0.059$) of the variation, with the vaults of older animals demonstrating increased postorbital constriction, a protruding glabellar region, an anterior flattening, and a particularly pointy inionic region.

Only CS has a significant effect on cranial base shape variation. A modest 2.5% ($P = 0.006$) of the total cranial base variation is size-related and an insignificant 1.4% ($P = 0.12$) is age-related. The major effect of allometry is a vertical compression of the basicranium in larger individuals. In contrast, age has the effect of rotating the basicranium with the fulcrum essentially located at the landmark OPI. The result is an occipital bone that is tilted backward along its superior margin at the nuchal crest, external auditory meati that extend posteriorly, a foramen magnum that is displaced superiorly at its anterior margin, and a less flexed posterior cranial base (i.e., a more horizontally positioned basioccipital).

Finally, the facial skeleton is affected to varying degrees by all three independent variables. Of the total facial variation, CS accounts for 9.9% ($P = 0.001$), age for 3.8% ($P = 0.001$), and tooth loss for 1.3% ($P = 0.066$). Older individuals have a longer snout that is also wider across the anterior palate than their younger conspecifics. Large individuals also have a longer snout, but there is no difference in width when compared to smaller individuals. Both advanced age and increased size are associated with a more narrow upper face, but this is due to a disproportionate decrease in the width of the fronto-zygomatic

process in older individuals, whereas it is the width of the orbit itself that is reduced in large individuals. The glabellar and supraorbital regions are only variable along the age axis, with both increasing in prominence in older individuals. The maxillary dentition is placed more anteriorly in large and old individuals relative to small and young ones. However, the allometric trend affects the entire oral cavity, displacing both the palate and dentition forward, while age alters the depth of the palate, the relationship between the palate and maxillary teeth, and the angle between the palate and the bones comprising the posterior nasopharynx.

4. Discussion

Much research has been conducted to describe patterns of growth and development in ontogenetic series of non-human primates, but the effect of post-maturational aging on the CFS remains understudied. Researchers are well aware that cranial morphology changes, often drastically, before individuals reach sexual maturity (e.g., in *Papio*: Leigh and Cheverud, 1991; Collard and O'Higgins, 2001; Singleton, 2012). Consequently, such ontogenetic patterns are typically accounted for, or at least acknowledged, in studies of both extant and fossil taxa. However, research on modern and historic geriatric human samples and on a select few non-human primate populations indicates that portions of the CFS demonstrate age-related changes in mature individuals. Our data add to this body of literature by demonstrating age-related craniofacial variation in a sample of sexually mature female baboons.

We suggest the combination of our data and those presented in the literature lends support to the idea that there exists in primates a more general post-maturational aging pattern that has heretofore been inadequately studied. Whether such a pattern extends to other mammalian orders largely remains to be seen, although there is some evidence for variation in both adolescent and post-maturational growth patterns of the carnivoran CFS, with some felid genera developing past the age of sexual maturity (e.g., Segura and Prevosti,

2012; Segura et al., 2013; Segura, 2015).

Surprisingly, our data do not document a significant degree of tooth loss-related modification of the midface and palate. Primarily, we observed morphological change near muscle attachment sites of the CFS and in individuals who retain all their teeth. These results suggest that the age-category "adult" is heterogeneous and we should be aware that it encompasses individuals demonstrating the effects of age on their CFS, regardless of their dental status.

4.1. Allometric patterns and how they differ from age-related ones

When visualizing the age- and size-related changes in the female baboon CFS, it appears that some of the regions experiencing the biggest shape changes are the same in both cases (see Fig. 4). However, there are subtle differences between the two. For example, the patterns of large-scale increase in facial length differ when considering solely age- or size-related variation. The snout of older individuals is primarily elongated in the sagittal plane only. In contrast, allometry displaces the premaxilla obliquely, both forward and downward. Additionally, with the major exception of the neurocranium, which is more globular in small females and narrows with increasing size, form differences associated with allometry are almost exclusively the result of increase in size of various cranial dimensions (i.e., osteoblastic activity on ectocranial surfaces coupled with osteoclastic activity on endocranial ones). The same cannot be said for age-related shape variation, which appears to result from osteoclastic activity on both endo- and ectocranial surfaces. The most obvious example of this difference is the midfacial remodeling of older females, which produces a marked concavity that is not seen in younger individuals and does not differ between small and large individuals.

As many of the regions showing localized differences between small and large crania are where major muscles attach (e.g., nuchal crest, inferior zygomatic arch, temporal surface, and pterygoid plates), it seems reasonable to suggest that an allometric increase in muscle mass with increasing body size (e.g., Alexander et al., 1981; Pollock and Shadwick, 1994)

may contribute to size-related variation in the CFS. Because the variance in adult male baboon body weight (27.01 ± 4.72 kg, $N = 247$; Leigh, 2009) is significantly greater ($F = 0.513, P < 0.0001$) than that of females (15.96 ± 3.38 kg, $N = 215$; Leigh, 2009), we would expect allometry to account for a larger proportion of craniofacial variation in a dataset of adult male baboons that was analyzed in a comparable manner to our present analysis of adult female baboons. Additionally, given that (a) numerous studies have identified sexual dimorphism in patterns of age-related variation of human and non-human primate CFS (e.g., Wang et al., 2007; Williams and Slice, 2010; Balolia et al., 2013) and (b) sexual dimorphism in both cranial size and shape is extremely large in baboons (e.g., Leigh and Cheverud, 1991; O'Higgins and Collard, 2002; Singleton, 2002), we could expect to identify different patterns of age-related variation in adult male baboon crania than those we have observed in females.

The remaining hot-spot not related to a muscle attachment site on the size-related panel of Figure 4 is the anterior rostrum. This is the same region that is highly sexually dimorphic in baboons (e.g., Leigh, 2006; Collard and O'Higgins, 2001; Singleton, 2002). As males are also significantly larger than females in body size (e.g., Leigh, 2009), it is not surprising that the crania of larger females appear more "male-like" in having a relatively long snout. This supports the suggestion that the extreme prognathism of *Papio* and its sister taxon *Mandrillus*, is related to their increased body size relative to smaller-bodied papionins, such as *Macaca, Cercocebus,* and *Lophocebus*. We were able to test for co-variation between body and cranial size in our sample of female baboons because longitudinal body weight records were collected opportunistically from birth to 15 years of age (see Joganic et al., 2018, for more details). Female adult body weight explains a significant 14.8% (OLS: $F = 17.7, P < 0.0001$) of the variation in overall CFS centroid size and a varying amount of the variation within each region (face: $R^2 = 0.171, P < 0.0001$; base: $R^2 = 0.124, P = 0.0003$; vault: $R^2 = 0.054, P = 0.02$). In female baboons at least, these findings are consistent with the

hypothesis of Joganic et al. (2018), which posits that larger-bodied papionin species tend to have similar-looking longer faces because approximately 15% of the genetic variation underlying morphological variation in both body size and CFS shape is shared.

4.2. Age-effects are global but differ by region in magnitude

According to Israel (1973a), human crania exhibit "virtual magnification," whereby the percent size increase (5–7%) is uniform and symmetrical across regions as adults age. The only exceptions he identified were in the sizes of the sella turcica (9–22%) and paranasal sinuses (7–12%) and in cranial vault thickness (1–11%). All other dimensions demonstrated less gain (0–5%). We found a subtly different pattern in our sample of female baboons (Supp. Fig. S4). The centroid size of both the cranial vault and base increased 1.8% and 1.5%, respectively, while in the facial skeleton it increased 3.3%. Even though the differences are slight, we suggest they may reflect what we know of baboon biology. Most of the ontogenetic change that occurs late in the CFS is primarily in the face, particularly the lengthening of the snout, especially in males (e.g., Collard and O'Higgins, 2001; Leigh, 2006). Although the focus in the literature is primarily on the effect that this phenomenon has on the male CFS, our results suggest that it may be relevant when considering female cranial morphology as well.

Most of the age-related changes we observed in our sample are concentrated in the facial skeleton, although the nuchal region is affected also (Fig. 5*a*–5*d*). As sutural fusion and subsequent obliteration likely prevent depositional growth at sutural margins, especially in the cranial vault and basicranium (see Opperman, 2000 for a review), the size and shape variation associated with increasing age in our sample are likely the result of appositional growth along ectocranial surfaces. In some regions, such as the midsagittal profile of the superior neurocranium, this is coupled with endocranial resorption that serves to maintain the same cranial vault thickness in YA and older age groups. Other areas, such as the supraorbital and inionic regions, experience a disproportionate degree of ectocranial deposi-

tion relative to endocranial resorption (remodeling), resulting in a thickening of the involved cranial bones (see Fig. 5*e*).

[Figure 5 about here.]

4.3. Potential role for extended ontogenetic trajectories

Previous research in baboons has suggested skeletal growth, including upper facial height and cranial length, generally ceases in females by the age of 5 years (Leigh, 2009), around the time when sexual maturity is achieved (Altmann et al., 1981). Our data provide an opportunity to more thoroughly test this hypothesis, as well as to examine potential changes in shape that may occur in the CFS of female baboons after this age. We found that female baboon cranial shape changes and its size increases between young adulthood (ages 7–16 years) and older age (> 18 years).

Our results raise interesting questions about the potential for various intrinsic and extrinsic factors to pattern variation in the post-maturational CFS. Due to large canine size, especially in males, canine development is relatively extended in baboons. Research on mandibular teeth in captive baboons by Swindler and Meekins (1991) demonstrates that time from initial crown calcification to apical closure in canines is ∼5.5 years, while for all other tooth types it ranges from 2.4–3.7 years. However, despite this prolonged canine development, the size and shape changes we have observed in the YA female face cannot be linked to anterior dental development because maxillary canine length has reached its adult size by 5 years of age in captive females (Table 5) and apical closure, at least of the mandibular canine, occurs by 6.3 years of age (Swindler and Meekins, 1991). Although age at apical closure for the maxillary dentition is unknown, age at eruption for the maxillary (4.1 years) and mandibular (3.9 years) canines differs by very little (Phillips-Conroy and Jolly, 1988), so it stands to reason that apical closure of the maxillary canine is also not more than a few months later than that of the mandibular canine.

[Table 5 about here.]

Size and shape change of the CFS of young adult female baboons also cannot be attributed to the appearance of the last tooth to erupt, the M3, which occurs at ages 6.2 (mandibular) and 7.1 (maxillary) years in captive females (Phillips-Conroy and Jolly, 1988), because eruption proceeds in a very rapid manner. In captive males, the mandibular M3 erupts at 6.3 years and apical closure is achieved by 6.5 years (Swindler and Meekins, 1991). Although this M3 completion time is only for mandibular teeth in males, there is no evidence to suggest estimates of the length of time between eruption and apical closure in maxillary teeth differs from that of mandibular teeth. Additionally, evidence from humans, macaques, and baboons demonstrates that the general trend is for teeth to develop slightly earlier in males but more rapidly in females, such that female dental development is actually completed earlier than that of males (e.g., Garn et al., 1958; Swindler and Meekins, 1991; Swindler et al., 1982). Finally, although Swindler and Meekins (1991) did not have enough individuals to provide estimates of variation in age at apical closure for the mandibular M3, the range of standard deviation estimates for the other tooth types is 0.13–0.54 years. Therefore, all forces that may be exerted by dental eruption on the CFS cease before individuals are ~7.5 years old. Yet, the female baboon CFS increases in size by 2.4% and changes shape between the ages of 7 and 16.

The fact that the greatest differences are between the YA group and all older baboons lends indirect support to the idea that growth in the CFS may not cease upon achieving sexual maturity. It is interesting to note that the late-stage ontogenetic patterns in *Pan* cranial development identified by Mitteroecker et al. (2004b) (to include a superior shift of the nuchal plane, an elongation of the anterior midface, and an enlargement of the torus supraorbitalis) appear remarkably similar to the differences between YA and older baboons that we have observed. Furthermore, Balolia et al. (2013) demonstrate continued growth of the CFS in young adults of multiple species of non-human primates, which they interpret

to be an extension of ontogenetic trajectories into adulthood. However, without a complementary ontogenetic sample in which to measure growth vectors to determine if the shape changes prior to achieving sexual maturity parallel those following it, we cannot definitively determine if the patterns we have observed are the result of ontogeney extending into "adulthood."

On the other hand, if future research demonstrates that the developmental trajectories of ontogenetic and adult samples of baboons are divergent, it is less likely that changes in the adult CFS are the result of either intrinsic growth mechanisms or the influence of adaptive growth centers that accommodate change among adjacent cranial components during ontogeny. Rather, it is more likely that factors that respond to extrinsic environmental cues, such as ambient temperature, stress and strain from muscular activity, and idiosyncratic behaviors, may play more pivotal roles in structuring adult craniofacial variation. It is also possible that, as has been shown in human research (e.g., Crothers and Sandham, 1993; Johansson et al., 1993), both dental wear and intra-population variation in dental wear could contribute to observable differences in the CFS of adult baboons. However, it may be difficult to disentangle the effects related to dental wear and those related to increased usage of masticatory musculature, which also has been shown to pattern CFS shape and is often the cause of excessive dental wear (e.g., Krogstad and Dahl, 1985; Waltimo et al., 1994; Kiliaridis, 1995; Kiliaridis et al., 1995).

4.4. The effects of mastication on the aging baboon cranium

Oyen et al. (1979) developed a model for *Papio* browridge formation positing that cyclical deposition of supraorbital bone as a response to recurrently increased masticatory stress produces the distinctive torus seen in adult baboons, particularly males. With the eruption of each new permanent post-canine tooth, the maxilla is repeatedly displaced anteriorly (Oyen, 1984). This lengthens the load arm of the TMJ, thus theoretically decreasing the biomechanical efficiency of the entire masticatory apparatus. However, subsequent research

demonstrates that very little strain is actually experienced in the circumorbital region (e.g., Hylander et al., 1991; Ross and Metzger, 2004), although Dechow et al. (2010) did observe thinner cortical bone with reduced directional orientation across the cranium and including the browridge, suggesting that masticatory forces do play a role in maintaining CFS bone mass. Dechow and Carlson (1990) directly tested Oyen's model by conducting biomechanical and comparative anatomical analyses in immature and adult macaques, phylogenetic cousins of baboons. They were able to demonstrate that the mechanical advantage of the masticatory muscles considered (masseter and temporalis) actually increased 7–14% for molar biting between juvenile and sexually mature individuals. As their muscle force data suggest that adult macaques actually have more efficiently placed masseters, they argue that the biomechanial model of Oyen (1984) is invalid. Dechow and Carlson (1990) suggest their unexpected results are either due to a disproportionate growth in the anterior portion of the muscle or a mechanically advantageous shift in how the teeth are positioned relative to muscle attachment sites.

We observed both an anterior displacement of the teeth relative to the zygomaxillary suture (the anterior-most extent of the superficial masseter origin) and a posterior displacement of the zygomatic bone itself with little relative movement of the glenoid fossa (see Fig. 5*f*). According to the biomechanical model presented by Dechow and Carlson (1990, Fig. 2), these changes in facial architecture as adults age should have an effect on masticatory efficiency. The result would be an increased molar biting moment (load) arm and a decreased masseter muscle moment (lever) arm. As mechanical advantage of a muscle is defined as the ratio between lever and load arms, the change in facial configuration from the YA to older age categories should have the effect of decreasing superficial masseter efficiency, as suggested by Oyen (1984). An additional issue to be considered is that increasing tooth wear and the potential for changes in manidbular ramus height as individuals age can alter masseter orientation, thus affecting its action and potentially its efficiency, as well. Although

anatomical arrangement of macaque and baboon masticatory musculature is incredibly similar (JLJ, pers. obs.; Schwartz and Huelke, 1963), the baboon facial skeleton is much more prognathic than that of macaques, which may explain the discrepancy between the results of Oyen (1984) and those of Dechow and Carlson (1990).

Our morphological data suggest that, even though the age-effects we have observed in adult female baboons are small in magnitude, the associated CFS size and shape changes occur in regions with the potential to impact masticatory behavior. However, biomechanical analyses on the baboon masticatory system need to be conducted to test whether muscular advantage changes over the course of both adolescent growth and post-maturational size and shape change. If future research is able to demonstrate that even subtle morphological change in adult craniofacial structure, such as the shape variation we have identified in our data, potentially alters masticatory effeciency, then the resulting modification to biomechanical loading regimes could induce additional changes in the CFS, as Oyen et al. (1979) suggest (see also Kiliaridis 1995). In fact, the subtle decrease in orbital circumference that is visible along the superior orbital margin may be a manifestation of changes in the masticatory complex. Alternatively, it could be related to the fact that the frontal sinus enlarges with age, which may influence age-related changes in the shape of the orbits (Fatu et al., 2006). Much more work needs to be done to determine whether such intraindividual variation has the potential to affect evolutionary fitness over the course of an individual's lifetime.

Finally, modifications in craniofacial configuration are not only observed in relation to morphological features associated with mastication. The other main feature that distinguishes YA and older crania is the increasing prominence of the inionic region as individuals age (see Fig. 5*a*). Interestingly, despite having absolutely larger muscles, large individuals do not have an appreciably more developed inion than their smaller conspecifics. This indicates that allometric shape differences may help larger animals withstand the increased force gen-

erated by larger muscles, but not necessarily their repetitive actions. As an indirect method of testing this hypothesis, we compared the mean difference in shape between five each of the smallest YA and older individuals and between five each of the largest YA and older individuals. Shape was quantified as an individual's regression score from the multivariate regression of PSCs on age. Although the larger individuals are located in a different area of the morphospace (average regression scores for small: $\bar{X}_{YA} = -0.0248, \bar{X}_{pooled} = -0.0065$; large: $\bar{X}_{YA} = -0.0066, \bar{X}_{pooled} = 0.0130$; Supp. Fig. S5), the amount of shape difference between the younger and older individuals (small: 0.0183, large: 0.0196) is essentially the same in both size categories.

These results, coupled with the observed pattern of shape change in the adult CFS, suggest that bone remodeling in response to cyclical bone strain from repetitive muscle use over the course of an individual's life is potentially a major factor in patterning age-related changes in craniofacial form in adult female baboons, regardless of the size of either the individual or their masticatory muscles. Given that age-related shape change appears to be concentrated at muscle attachment sites, including the nuchal region, we propose that future research should aim to further our knowledge of cranial-postcranial integration. Vertebral anatomy and its relationship to basicranial anatomy and posture in primates is the subject of some research (e.g., Russo and Kirk, 2013; Nalley and Grider-Potter, 2015; Villamil, 2018), but our results demonstrate that its effect on cranial vault anatomy via the link with the nuchal musculature should be assessed as well.

5. Conclusion

We have demonstrated that the size and shape of the CFS in female baboons change moderately past the age of sexual maturity and into early adulthood. Contrary to expectations based on previous knowledge about the effects of tooth loss and accompanying alveolar resorption, it is actually the YA category that is most different from the other age groups.

Younger and older adults differ most in regions related to muscle attachment sites, suggesting a possible role for repetitive masticatory stress in patterning bone remodeling in the adult CFS. The facial skeleton experiences the greatest amount of age- and size-related change. A complementary and detailed geometric morphometric study of post-maturational modifications in the human CFS could provide insight into mechanisms of aging that are shared or differ across primate taxa.

Acknowledgements

Funding for specimen curation at Washington University in St. Louis and CT scan acquisition at the Washington University School of Medicine Mallinckrodt Institute of Radiology was provided by NSF BCS-0725068 and BCS-0523637. This study received financial support from the French State in the framework of the "Investments for the Future" Program, IdEx Bordeaux (ANR-10-IDEX-03-02). Anthony Comuzzie and Michael Mahaney provided access to the body weight data from the Southwest National Primate Research Center. Frédéric Santos and Kathryn Trinkaus provided valuable statistical advice and the comments of David Strait and four anonymous reviewers greatly improved early versions of the manuscript. Neither author has a conflict of interest to declare.

Author Contributions

Jessica Joganic: project conception and design, data acquisition and analysis, results interpretation, manuscript drafting and revision. Yann Heuzé: project conception and design, results interpretation, manuscript revision.

References

Adams DC, Collyer ML, Kaliontzopoulou A, 2018. Geomorph: software for geometric morphometric analyses. R package version 3.0.6.
URL https://cran.r-project.org/package=geomorph.

Albert AM, Ricanek K, Patterson E, 2007. A review of the literature on the aging adult skull and face: implications for forensic science research and applications. Forensic Sci Int 172, 1–9.

Alexander RM, Jayes AS, Maloiy GMO, Wathuta EM, 1981. Allometry of the leg muscles of mammals. J Zool Lond 194, 539–52.

Altmann J, Altmann S, Hausfater G, 1981. Physical maturation and age estimates of yellow baboons, *Papio cynocephalus*, in Amboseli National Park, Kenya. Am J Primatol 1, 1389–399.

Balolia KL, 2015. Brief communication: the timing of spheno-occipital fusion in hominoids. Am J Phys Anthropol 156, 135–40.

Balolia KL, Soligo C, Lockwood CA, 2013. Sexual dimorphism and facial growth beyond dental maturity in great apes and gibbons. Int J Primatol 34, 361–87.

Bartlett SP, Grossman R, Whitaker LA, 1992. Age-related changes of the craniofacial skeleton: an anthropometric and histologic analysis. Plast Reconstr Surg 90, 592–600.

Bastir M, Rosas A, O'Higgins P, 2006. Craniofacial levels and the morphological maturation of the human skull. J Anat 209, 637–654.

Begg PR, 1954. Stone Age man's dentition: with reference to anatomically correct occlusion, the etiology of malocclusion, and a technique for its treatment. Am J Orthod 40, 298–312.

Behrents RG, 1985. Growth in the aging craniofacial skeleton. Ph.D. thesis, University of Michigan, Ann Arbor.

Biewener AA, Bertram JEA, 1993. Mechanical loading and bone growth *in vivo*. In: Hall BK (Ed.), Bone. Volume 7: Bone Growth–B. CRC Press, Boca Raton, FL, Ch. 1, pp. 1–36.

Bondevik O, 1995. Growth changes in the cranial base and the face: a longitudinal cephalometric study of linear and angular changes in adult Norwegians. Eur J Orthod 17, 525–532.

Bookstein FL, 1996. Combining the tools of geometric morphometrics. In: Advances in Morphometrics. Springer US, Boston, MA, pp. 131–151.

Boskey AL, Coleman R, 2010. Aging and bone. J Dent Res 89, 1333–1348.

Bramblett CA, 1969. Non-metric skeletal age changes in the Darajani baboon. Am J Phys Anthropol 30, 161–71.

Cheverud JM, 1982. Phenotypic, genetic, and environmental morphological integration in the cranium. Evol 36, 499–516.

Cheverud JM, 1995. Morphological integration in the saddle-back tamarin (*Saguinus fuscicollis*) cranium. Am Nat 145, 63–89.

Collard M, O'Higgins P, 2001. Ontogeny and homoplasy in the papionin monkey face. Evol Dev, 322–331.

Colman RJ, Kemnitz JW, Lane MA, Abbott DH, Binkley N, 1999. Skeletal effects of aging and menopausal status in female Rhesus macaques. J Clin Endocrinol Metab 84, 4144–4148.

Crothers A, Sandham A, 1993. Vertical height differences in subjects with severe dental wear. Eur J Orthod 15, 519–25.

Currey JD, 1984. The mechanical adaptations of bones. Princeton University Press, Princeton, NJ.

Dechow PC, Carlson DS, 1990. Occlusal force and craniofacial biomechanics during growth in Rhesus monkeys. Am J Phys Anthropol 83, 219–237.

Dechow PC, Wang Q, Peterson J, 2010. Edentulation alters material properties of cortical bone in the human craniofacial skeleton: functional implications for craniofacial structure in primate evolution. Anat Rec Adv Integr Anat Evol Biol 293, 618–629.

Enlow DH, 1975. Handbook of facial growth. W. B. Saunders Company, Philadelphia, PA.

Falk D, Konigsberg L, Helmkamp RC, Cheverud J, Vannier M, Hildebolt C, 1989. Endocranial suture closure in rhesu macaques (*Macaca mulatta*). Am J Phys Anthropol 80, 417–28.

Fatu C, Puisoru M, Rotaru M, Truta AM, 2006. Morphometric evaluation of the frontal sinus in relation to age. Ann Anat 188, 275–280.

Formby WA, Nanda RS, Currier GF, 1994. Longitudinal changes in the adult facial profile. Am J Orthod Dentofac Orthop 105, 464–476.

Franklin D, Flavel A, 2014. Brief communication: timing of spheno-occipital closure in modern western Australians. Am J Phys Anthropol 153, 132–8.

Frost HM, 1969. Tetracycline-based histological analysis of bone remodeling. Calcif Tissue Res 3, 211–37.

Frost SR, Marcus LF, Bookstein FL, Reddy DP, Delson E, 2003. Cranial allometry, phylogeography, and systematics of large-bodied papionins (Primates: Cercopithecinae) inferred from geometric morphometric analysis of landmark data. Anat Rec A Discov Mol Cell Evol Biol 275, 1048–72.

Garn SM, Lewis AB, Koski K, Polacheck DL, 1958. The sex difference in tooth calcification. J Dent Res 37, 561–7.

Goodall C, 1991. Procrustes methods in the statistical analysis of shape. J R Stat Soc Ser B 53, 285–339.

Guagliardo MF, 1982. Craniofacial structure, aging and dental function: their relationships in adult human skeletal series. Ph.D. thesis, University of Tennessee, Knoxville.

Gunz P, Mitteroecker P, 2013. Semilandmarks: a method for quantifying curves and surfaces. Hystrix Ital J Mammal 24, 103–109.

Hellman M, 1927. Changes in the human face brought about by development. Int J Orthod Oral Surg Radiogr 13, 475–516.

Hens SM, 2005. Ontogeny of craniofacial sexual dimorphism in the orangutan (*Pongo pygmaeus*). i: face and palate. Am J Primatol 65, 149–66.

Herzberg F, Holic R, 1943. An anthropologic study of face height. Am J Orthod Oral Surg 29, 90–100.

Heuzé Y, Boyadjiev SA, Marsh JL, Kane AA, Cherkez E, Boggan JE, Richtsmeier JT, 2010. New insights into the relationship between suture closure and craniofacial dysmorphology in sagittal nonsyndromic craniosynostosis. J Anat 217, 85–96.

Heuzé Y, Martínez-Abadías N, Stella JM, Arnaud E, Collet C, García Fructuoso G, Alamar M, Lo LJ, Boyadjiev SA, Di Rocco F, Richtsmeier JT, 2014. Quantification of facial skeletal shape variation in fibroblast growth factor receptor-related craniosynostosis syndromes. Birth Defects Res Part A Clin Mol Teratol 100, 250–259.

Hooton EA, Dupertuis CW, 1951. Age changes and selective survival in Irish males. Edwards Brothers, Inc., Ann Arbor, MI.

Hrdlička A, 1925. The old Americans. Williams & Wilkins, Baltimore, MD.

Hylander WL, Picq PG, Johnson KR, 1991. Function of the supraorbital region of primates. Arch Oral Biol 36, 273–81.

Israel H, 1968. Continuing growth in the human cranial skeleton. Arch Oral Biol 13, 133–137.

Israel H, 1973a. Age factor and the pattern of change in craniofacial structures. Amer J Phys Anthropol 39, 111–128.

Israel H, 1973b. Recent knowledge concerning craniofacial aging. Angle Orthod 43, 176–184.

Israel H, 1977. The dichotomous pattern of craniofacial expansion during aging. Am J Phys Anthropol 47, 47–51.

Jaul DH, McNamara JA, Carlson DS, Upton LGS, 1980. A cephalometric evaluation of edentulous Rhesus monkeys (*Macaca mulatta*): A long-term study. J Prosthet Dent 44, 453–460.

Joganic JL, Willmore KE, Richtsmeier JT, Weiss KM, Mahaney MC, Rogers J, Cheverud JM, 2018. Additive genetic variation in the craniofacial skeleton of baboons (genus *Papio*) and its relationship

to body and cranial size. Am J Phys Anthropol 165, 269–285.

Johansson A, Kiliaridis S, Haraldson T, Omar R, Carlsson GE, 1993. Covariation of some factors associated with occlusal tooth wear in a selected high-wear sample. Eur J Oral Sci 101, 398–406.

Kiliaridis S, 1995. Masticatory muscle influence on craniofacial growth. Acta Odontol Scand 153, 196–202.

Kiliaridis S, Johansson A, Haraldson T, Omar R, Carlsson GE, 1995. Craniofacial morphology, occlusal traits, and bite force in persons with advanced occlusal tooth wear. Am J Orthod Dentofac Orthop 107, 286–92.

Klingenberg CP, 2011. MorphoJ: An integrated software package for geometric morphometrics. Mol Ecol Resour 11, 353–357.

Klingenberg CP, 2016. Size, shape, and form: concepts of allometry in geometric morphometrics. Dev Genes Evol 226, 113–137.

Krogstad O, Dahl BL, 1985. Dento-facial morphology in patients with advanced attrition. Eur J Orthod 7, 57–62.

Larsen CS, 1995. Biological changes in human populations with agriculture. Annu Rev Anthropol 24, 185–213.

Lasker G, 1953. The age factor in bodily measurements of adult male and female Mexicans. Hum Biol 25, 50–63.

Legan HL, Nanda R, 1978. Craniofacial adaptations after total maxillary osteotomy in *Macaca irus*: A cephalometric and histologic study. Am J Orthod 73, 410–427.

Leigh SR, 2006. Cranial ontogeny of Papio baboons (*Papio hamadryas*). Am J Phys Anthropol 130, 71–84.

Leigh SR, 2009. Growth and development of baboons. In: VandeBerg JL, Williams-Blangero S, Tardif SD (Eds.), The baboon in biomedical research. Springer-Verlag New York, New York, NY, Ch. 3, pp. 57–88.

Leigh SR, Cheverud JM, 1991. Sexual dimorphism in the baboon facial skeleton. Am J Phys Anthropol 84, 193–208.

Levine RA, Garza JR, Wang PTH, Hurst CL, Dev VR, 2003. Adult facial growth: applications to aesthetic surgery. Aesth Plast Surg 27, 265–268.

Lieberman DE, 2008. Speculations about the selective basis for modern human craniofacial form. Evol Anthropol 17, 55–68.

Lieberman DE, Krovitz GE, Yates FW, Devlin M, St. Claire M, 2004. Effects of food processing on masticatory strain and craniofacial growth in a retrognathic face. J Hum Evol 46, 655–677.

Litsas G, 2015. Growth hormone and craniofacial tissues. An update. Open Dent J 9, 1–8.

Maples WR, McKern MA, McKern TW, 1967. A preliminary report on classification of the Kenya baboon. In: Vagtborg H (Ed.), The baboon in biomedical research, vol II: proceedings of the second international symposium on the baboon and its use as an experimental animal. University of Texas Press, Austin, TX, pp. 13–22.

Matros E, Momoh A, Yaremchuk MJ, 2009. The aging midfacial skeleton: implications for rejuvenation and reconstruction using implants. Facial Plast Surg 25, 252–259.

Mendelson B, Wong CH, 2012. Changes in the facial skeleton with aging: implications and clinical applications in facial rejuvenation. Aesth Plast Surg 36, 753–760.

Mendelson BC, Hartley W, Scott M, McNab A, Granzow JW, 2007. Age-related changes of the orbit and midcheek and the implications for facial rejuvenation. Aesthetic Plast Surg 31, 419–423.

Minh NV, Mouri T, Hamada Y, 2015. Aging-related changes in the skulls of Japanese macaques (*Macaca fuscata*): effect of the fragmentation on genetic diversity of macaque populations in the Central Vietnam View project. Anthropol Sci 123, 107–119.

Mitteroecker P, Gunz P, 2009. Advances in geometric morphometrics. Evol Biol 36, 235–247.

Mitteroecker P, Gunz P, Bernhard M, Schaefer K, Bookstein FL, 2004a. Comparison of cranial ontogenetic trajectories among great apes and humans. J Hum Evol 46, 679–98.

Mitteroecker P, Gunz P, Bookstein FL, 2005. Heterochrony and geometric morphometrics: a comparison of cranial growth in *Pan paniscus* verus *Pan troglodytes*. Evol Develop 7, 244–58.

Mitteroecker P, Gunz P, Weber GW, Bookstein FL, 2004b. Regional dissociated heterochrony in multivariate analysis. Ann Anat 186, 463–70.

Mundfrom DJ, Perrett JJ, Schaffer J, Piccone A, Roozeboom M, 2006. Bonferroni adjustments in tests for regression coefficients. Multiple Linear Regression Viewpoints 32, 1–6.

Nalley TK, Grider-Potter N, 2015. Functional morphology of the primate head and neck. Am J Phys Anthropol 156, 531–42.

O'Higgins P, Collard M, 2002. Sexual dimorphism and facial growth in papionin monkeys. J Zool Lond 257, 255–72.

Opperman LA, 2000. Cranial sutures as intramembranous bone growth sites. Develop Dynam 219, 472–485.

Oyen OJ, 1984. Palatal Growth in Baboons (*Papio cynocephalus anubis*). PRIMATES 25, 337–351.

Oyen OJ, Walker AC, Rice RW, 1979. Craniofacial growth in olive baboons (*Papio cynocephalus anubis*): browridge formation. Growth 43, 174–87.

Pessa JE, Zadoo VP, Mutimer KL, Haffner C, Yuan C, Dewitt AI, Garza JR, 1998. Relative maxillary retrusion as a natural consequence of aging: combining skeletal and soft-tissue changes into an integrated model of midfacial aging. Plast Reconstr Surg 102, 205–212.

Phillips-Conroy JE, Jolly CJ, 1988. Dental eruption schedules of wild and captive baboons. Am J Primatol 15, 17–29.

Poe DJ, 2011. Brief communication: testing the usefulness of the basilar suture as a means to determine age in great ape skeletons. Am J Phys Anthropol 14, 162–65.

Pollock CM, Shadwick RE, 1994. Allometry of muscle, tendon, and elastic energy storage capacity in mammals. Am J Physiol 266, R1022–31.

Porto A, de Oliveira FB, Shirai LT, de Conto V, Marroig G, 2009. The evolution of modularity in the mammalian skull I: morphological integration patterns and magnitudes. Evol Biol 36, 118–135.

Rafferty KL, Liu ZJ, Ye W, Navarrete AL, Nguyen TT, Salamati A, Herring SW, 2012. Botulinum toxin in masticatory muscles: short- and long-term effects on muscle, bone, and craniofacial function in adult rabbits. Bone 50, 651–662.

Ramfjord SP, Blankenship JR, 1981. Increased occlusal vertical dimension in adult monkeys. J Prosthet Dent 45, 74–83.

Rohlf FJ, Slice DE, 1990. Extensions of the Procrustes method for the optimal superimposition of landmarks. Syst Zool 39, 40–59.

Ross CF, Metzger KA, 2004. Bone strain gradients and optimization in vertebrate skulls. Ann Anat 186, 387–96.

Ruff CB, 1980. Age differences in craniofacial dimensions among adults from Indian Knoll, Kentucky. Am J Phys Anthropol 53, 101–108.

Russo GA, Kirk EC, 2013. Foramen magnum position in bipedal animals. J Hum Evol 65, 656–670.

Schlager S, 2017. Morpho and rvcg – shape analysis in R. In: Zheng G, Li S, Szekely G (Eds.), Statistical Shape and Deformation Analysis. Academic Press, London, UK, pp. 217–256.

Schwartz DJ, Huelke DF, 1963. Morphology of the head and neck of the macaque monkey: the muscles of mastication and the mandibular division of the trigeminal nerve. J Dent Res 42, 1222–1232.

Segura V, 2015. A three-dimensional skull ontogeny in the bobcat (*Lynx rufus*) (Carnivora: Felidae): a comparison with other carnivores. Can J Zool 93, 225–37.

Segura V, Prevosti F, 2012. A quantitative approach to the cranial ontogeny of *Lycalopex culpaeus* (Carnivora: Canidae). Zoomorphol 131, 79–92.

Segura V, Prevosti F, Cassini G, 2013. Cranial ontogeny in the Puma lineage, *Puma concolor*, *Herpailurus yagouaroundi*, and *Acinonyx jubatus* (Carnivora: Felidae): a three-dimensional geometric morphometric approach. Zool J Linnaean Soc 169, 235–50.

Shea BT, 1998. Post-natal craniofacial growth. In: Ulijaszek SJ, Johnston FE, Preece MA (Eds.), The Cambridge Encyclopedia of Human Growth and Development. Cambridge University Press, Cambridge, UK, Ch. 5.9, pp. 206–208.

Singleton M, 2002. Patterns of cranial shape variation in the Papionini (Primates: Cercopithecinae). J Hum Evol 42, 547–78.

Singleton M, 2012. Postnatal cranial development in papionin primates: an alternative model for hominin evolutionary development. Evol Biol 39, 499–520.

Sutton DN, Lewis BRK, Patel M, Cawood JI, 2004. Changes in facial form relative to progressive atrophy of the edentulous jaw. Int J Oral Maxillofac Surg 33, 676–682.

Swindler DR, Meekins D, 1991. Dental development of the permanent mandibular teeth in the baboon, *Papio cynocephalus*. Am J Hum Biol 3, 571–580.

Swindler DR, Olshan AF, Sirianni JE, 1982. Sex differences in permanent mandibular tooth development in *Macaca nemestrina*. Hum Biol 54, 45–52.

Tallgren A, 1974. Neurocranial morphology and ageing–a longitudinal roentgen cephalometric study of adult Finnish women. Am J Phys Anthropol 41, 285–293.

Todd TW, 1924. Thickness of the male white cranium. Anat Rec 27, 245–256.

United Nations, 2017. World population prospects: the 2017 revision, volume I: comprehensive tables. Tech. rep., UN Department of Economic and Social Affairs, Population Division.

Villamil CI, 2018. Phenotypic integration of the cervical vertebrae in the Hominoidea (Primates). Evol 72, 490–517.

Waltimo A, Nyström M, Kä nänen M, 1994. Bite force and dentofacial morphology in men with severe dental attrition. Eur J Oral Sci 102, 92–6.

Wang Q, Dechow PC, Hens SM, 2007. Ontogeny and diachronic changes in sexual dimorphism in the craniofacial skeleton of rhesus macaques from Cayo Santiago, Puerto Rico. J Hum Evol 53, 350–61.

Wang Q, Strait DS, Dechow PC, 2006. Fusion patterns of craniofacial sutures in rhesus monkey skulls of known age and sex from Cayo Santiago. Am J Phys Anthropol 131, 469–85.

Wei X, Hu M, Mishina Y, Liu F, 2016. Developmental regulation of the growth plate and cranial synchondrosis. J Dent Res 95, 1221–9.

Williams SE, Slice DE, 2010. Regional shape change in adult facial bone curvature with age. Am J Phys Anthropol 143, 437–447.

Wu M, Fannin J, Rice KM, Wang B, Blough ER, 2011. Effect of aging on cellular mechanotransduction. Ageing Res Rev 10, 1–15.

Wulc AE, Sharma P, Czyz CN, 2012. The anatomic basis of midfacial aging. In: Hartstein ME, Wulc AE, Holck DEE (Eds.), Midfacial Rejuvenation. Springer, New York, NY, pp. 15–28.

Xie Q, Wolf J, Ainamo A, 1997. Quantitative assessment of vertical heights of maxillary and mandibular bones in panoramic radiographs of elderly dentate and edentulous subjects. Acta Odontol Scand 55, 155–161.

Zihlman AL, Bolter DR, Boesch C, Zihlman AL, 2007. Skeletal and dental growth and development in chimpanzees of the Taï National Park, Côte D'Ivoire. J Zool 273, 63–73.

Zuckerman S, 1955. Age changes in the basicranial axis of the human skull. Amer J Phys Anthropol 13, 521–539.

Figure Legends

Figure 1: Craniometric landmarks, semilandmarks, and cranial regions. Locations of the craniometric landmarks color-coded by type: anatomical (black); orbital and zygomatic curve semilandmarks, SL (white); facial, vault, and occipital surface SL (pink); frontal surface SL (gold). Only the anatomical landmarks are identified and the corresponding abbreviations are provided in Table 2. Descriptions of anatomical features used to define the surface SL patches are provided in the text. The three anatomical regions are indicated by colored shading: face (green), base (yellow), and vault (lavender).

Figure 2: Centroid size boxplot. Comparison of centroid size distribution across age groups. Maximum: top whisker and number above it, 3rd quantile: top hinge, median: waist, confidence interval of the median: notch, mean: boldface number above the waist, standard deviation of the mean: italic typeface number below the waist, 1st quantile: bottom hinge, minimum: bottom whisker and the number below it. The confidence interval of the median is calculated as: $median \pm 1.58 \times \frac{IQR}{\sqrt{n}}$.

Figure 3: Growth maturation. Centroid size regressed on chronological age. Individuals are color-coded by age category, as indicated by the key in the top left corner. The OLS regression line is indicated with a solid black line and its formula and associated regression statistics are provided in the bottom right corner.

Figure 4: Vertex difference surface morphs. Heat maps of the distances between vectors comprising the triangular surface mesh of a small individual and the corresponding vectors of a large one (left panels) and between those of a young adult and the corresponding ones of an older individual (right panels). Regions shown in red are further apart between the two meshes than those shown in blue. In other words, these are areas that change the most with increasing age and size. Because the color scales are relative, the magnitude of the differences should not be compared between the allometric and age-related meshes.

Figure 5: Detailed depictions of age-related changes in the baboon CFS. In each panel, two surface meshes are superimposed. They were obtained by morphing the mean shape by the fitted regression coordinates for the youngest (pink mesh) and oldest (gray mesh) individuals from the multivariate regression of Procrustes shape coordinates (PSCs) on age. In panels *a b*, *d* and *f*, the young mesh is partially transparent; in panel *c*, it is the old mesh; and in panel *e*, both meshes are fully opaque. The symbols in each panel are as follows: (*a*) Green triangles, nuchal ligament and medial trapezius attachment; orange triangles, deep masseter attachment; magenta arrows, primary direction of lateral pterygoid muscle force and direction of pterygoid plate movement from youngest to oldest individuals. (*b*) Light blue triangle, anterior temporalis attachment; magenta triangles, lateral pterygoid attachment; gray arrows, direction of premaxillary change from youngest to oldest adult female baboons; colored arrows, primary direction of posterior face movement from youngest to oldest individuals and of muscle force for deep masseter (orange), anterior temporalis

(light blue), and superficial masseter and medial pterygoid (yellow). Note that the zygomatic arch has been cut away to enhance visualization. (*c*) Blue diamond, supraorbital ridge and glabella region; white triangle, posterior temporalis attachment. (*d*) Yellow triangles, superficial masseter attachment; arrows, concavity of the nasal bridge (light green) and midface (black) in the oldest individuals. (*e*) Gold line segment, cranial vault thickness in youngest individual; other line segments, old individual's cranial vault thickness when it is greater (purple) or less (lavender) than that of the youngest individual. (*f*) Open circles, anteromost extent of the malars; line segments, I1-M3 length; gold, young individual; purple, old individual.

Tables

Table 1: Sample demographics. Sample composition of the different age categories, the age ranges of included individuals in years, and the human equivalent age range, based on the worldwide average female human life expectancy of 73.1 years (United Nations, 2017).

Age Category	*N*	Mean (SD)	Min	Max	Human
Young Adult (YA)	25	11.56 (3.0)	7.12	16.20	15.7–35.8
Adult (AD)	25	20.00 (1.3)	17.97	22.55	39.7–49.9
Elderly (ER)	25	27.23 (2.5)	23.76	31.69	52.5–70.0
Tooth Loss (TL)	22	26.92 (2.3)	23.74	32.47	52.5–71.8

Table 2: Anatomical landmarks. Names, abbreviations, descriptions, and characteristics of the craniometric landmarks measured on female baboon crania.

Landmark	Symbol	Description	Region[1]	Located[2]
Inion	INI	Most posterior point in the midline of the nuchal crest, often on an inionic hook	V	M
Opisthion	OPI	Most posterior point on the foramen magnum's margin	B	M
Basion	BAS	Most anterior point on the foramen magnum's margin	B	M
Hormion	HOR	Junction of vomer's posterior border with the sphenoid	B	M
Posterior Nasal Spine	PNS	Most posterior point on the palate in the transverse plane	B	M
Incisive Canal	INC	Midline point on the incisive canal's posterior margin	F	M
Greater Palatine Foramen	GPF	Most posterior point on the greater palatine foramen's margin	F	B
Anterior Petrous Temporal	APT	Most anterior point on the ectocranial surface of the petrous temporal	B	B
Pterygomaxillary Septum	PMX	In the middle of the pterygomaxillary septum, or on the maxillary projection if the septum is incomplete	F	B
Stylomastoid Foramen	SMF	Most lateral point on the stylomastoid foramen's margin	B	B
Porion	POR	Anterior junction of the external auditory meatus and the nuchal crest	B	B
Zygotemporale Inferior	ZTI	Most inferior point on the zygotemporal suture	F	B
Frontomalar Foramen	FMF	Most inferior point on the frontozygomatic foramen's margin	F	B

Continued on next page

Table 2 – *Continued from previous page*

Landmark	Symbol	Description	Region[1]	Located[2]
Nasion	NAS	Intersection of the internasal suture and the frontal bone	F	M
Masseter Origin	MAS	Most anterior point on the inferior surface of the zygomatic arch where the masseter muscle originates	F	B
Nasomaxillare Inferior	NMI	Most anterior point on the nasomaxillary suture	F	B
Acanthion	ACN	Most anterior point on the nasal aperature's inferior margin	F	M
M3-M2 Septum	MM3	Most inferior point on the bony septum between upper M3 & M2	F	B
M2-M1 Septum	MM2	Most inferior point on the bony septum between upper M2 & M1	F	B
M1-P4 Septum	MM1	Most inferior point on the bony septum between upper M1 & P4	F	B
P4-P3 Septum	PM4	Most inferior point on the bony septum between upper P4 & P3	F	B
P3-CN Septum	PM3	Most posterior point on the upper canine alveolus	F	B
Premaxillary-maxillary Junction	PMM	Most anterior point on the superior premaxillary-maxillary suture	F	B
CN-I2	II2	Most distal point on the upper I2 alveolus	F	B
I2-I1	II1	Most inferior point on the bony septum between upper I2 & I1	F	B
Alveolare	ALV	Most inferior point on the bony septum between the upper I1's	F	M

[1]The region of the cranium in which the landmark is located: vault (V), base (B), face (F). [2]Whether the landmark is located in the midline (M) or bilaterally (B).

Table 3: Shape regression statistics. Type II MANOVA results from primary, dental, and region-specific shape regressions of Procrustes shape coordinates (PSCs) on centroid size (CS), age, and the number of teeth missing. The coefficient of determination (R^2), F-statistic, and P-value are provided for each independent variable included in the models. Values indicated in bold typeface are significant at an $\alpha = \frac{0.05}{3} = 0.017$, a Bonferroni correction applied to account for multiple comparisons *within* each model (Mundfrom et al., 2006).

Shape Reg.	Centroid Size			Age			Tooth Loss		
	R^2	F	P	R^2	F	P	R^2	F	P
Primary	**0.043**	**4.37**	**0.001**	**0.027**	**2.77**	**0.005**	0.010	1.02	0.317
Dental	0.082	1.90	0.041	0.036	0.83	0.392	0.090	2.08	0.038
Vault	**0.028**	**2.76**	**0.007**	0.018	1.73	0.059	0.005	0.45	0.939
Base	**0.025**	**2.49**	**0.006**	0.014	1.37	0.121	0.007	0.69	0.728
Face	**0.099**	**10.97**	**0.001**	**0.038**	**4.21**	**0.001**	0.013	1.46	0.066

Table 4: Procrustes distance matrix. Intergroup Procrustes distances (above the diagonal) and their significance based on permutation tests (below the diagonal). Distances that are significantly large at $\alpha = 0.05$ and their corresponding P-values are shown in bold typeface.

Age Group	Age Group			
	Young Adult	**Adult**	**Elderly**	**Tooth Loss**
Young Adult		**0.017**	**0.019**	**0.020**
Adult	**0.05**		0.010	0.012
Elderly	**0.02**	0.90		0.011
Tooth Loss	**0.02**	0.54	0.80	

Table 5: Female baboon canine growth. Maximum buccal length (mm) of the maxillary canines as measured from canine tip to gum line on anesthetized female baboons, from Leigh (2009).

Age (yrs)	*N*	Length (SD)	Age (yrs)	*N*	Length (SD)
3	2	2.05 (2.9)	10	4	9.65 (1.9)
4	21	8.30 (2.4)	11	5	11.94 (1.4)
5	28	10.37 (1.5)	12	2	9.10 (1.3)
6	17	10.25 (0.7)	16	2	8.80 (1.4)
7	8	10.73 (0.6)	19	2	9.60 (0.1)
8	5	11.65 (1.2)	20	2	12.70 (0.7)
9	3	10.72 (1.6)			

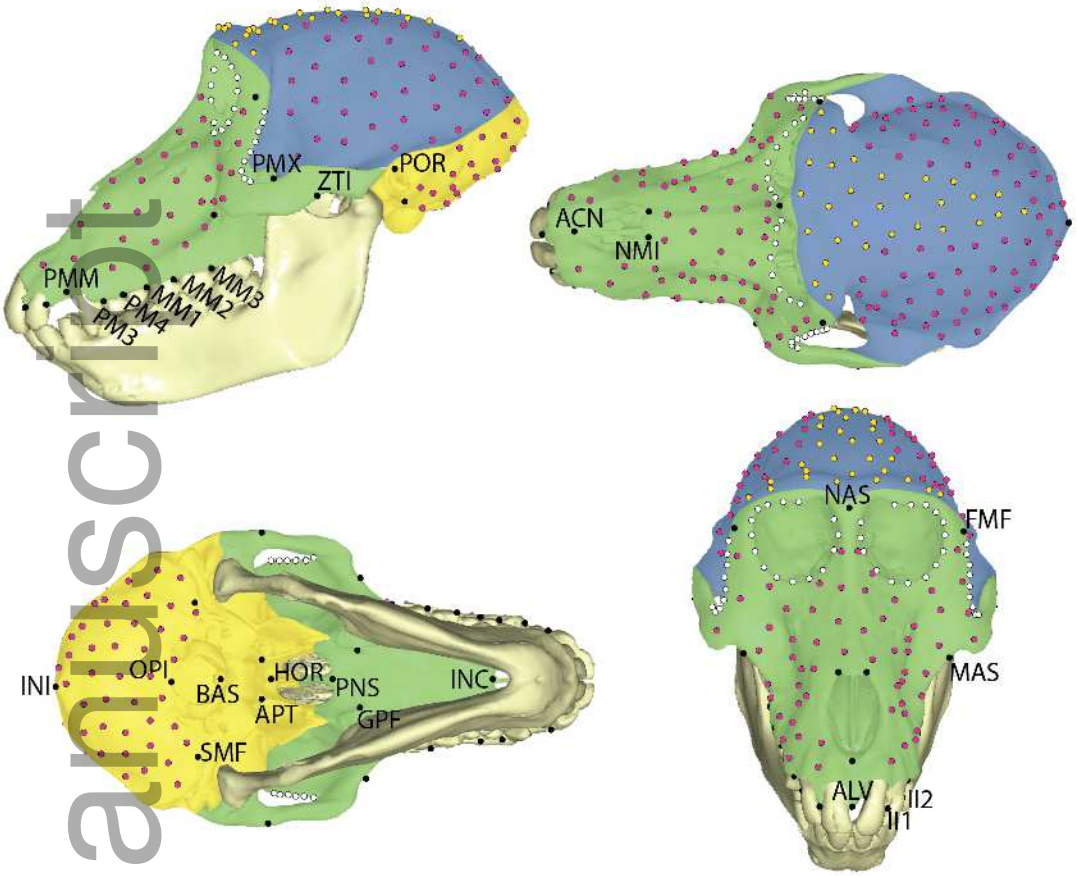

joa_13005_f1.png

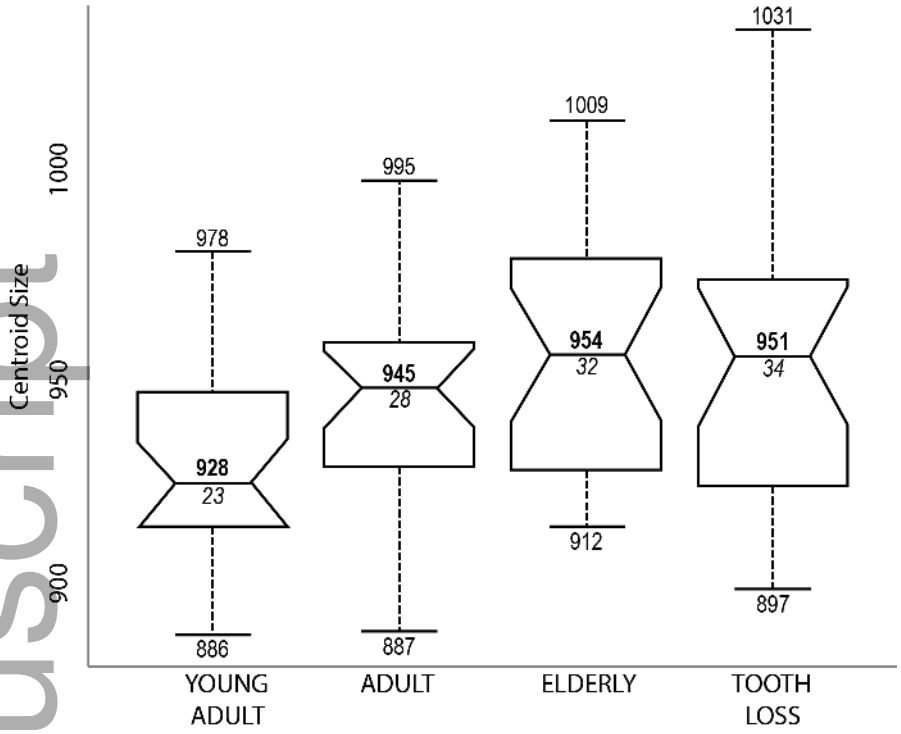

joa_13005_f2.png

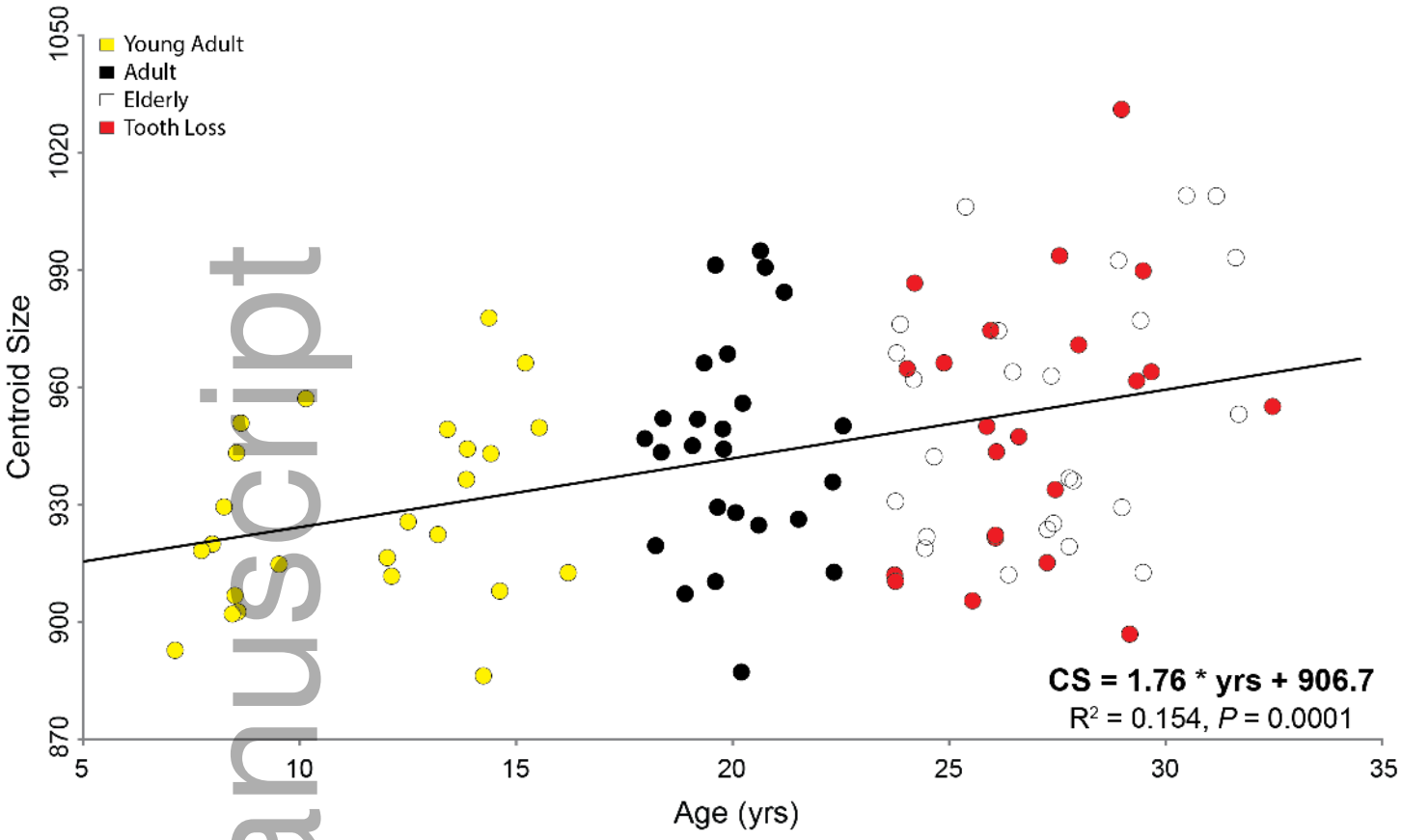

joa_13005_f3.png

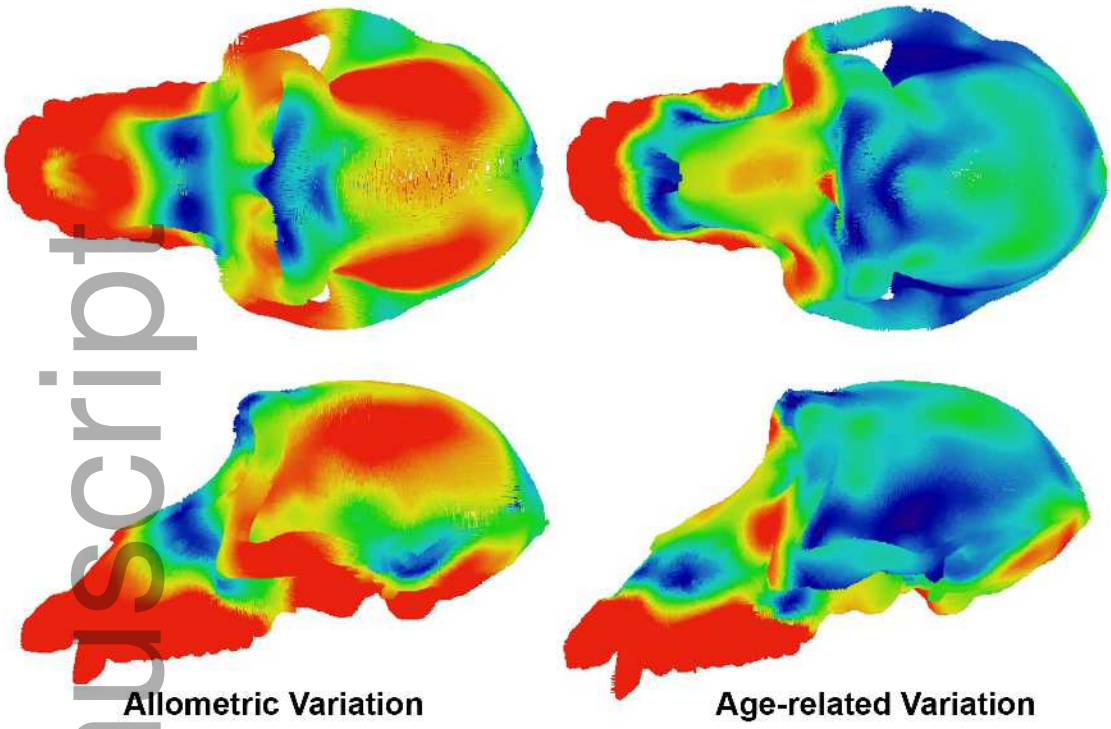

joa_13005_f4.png

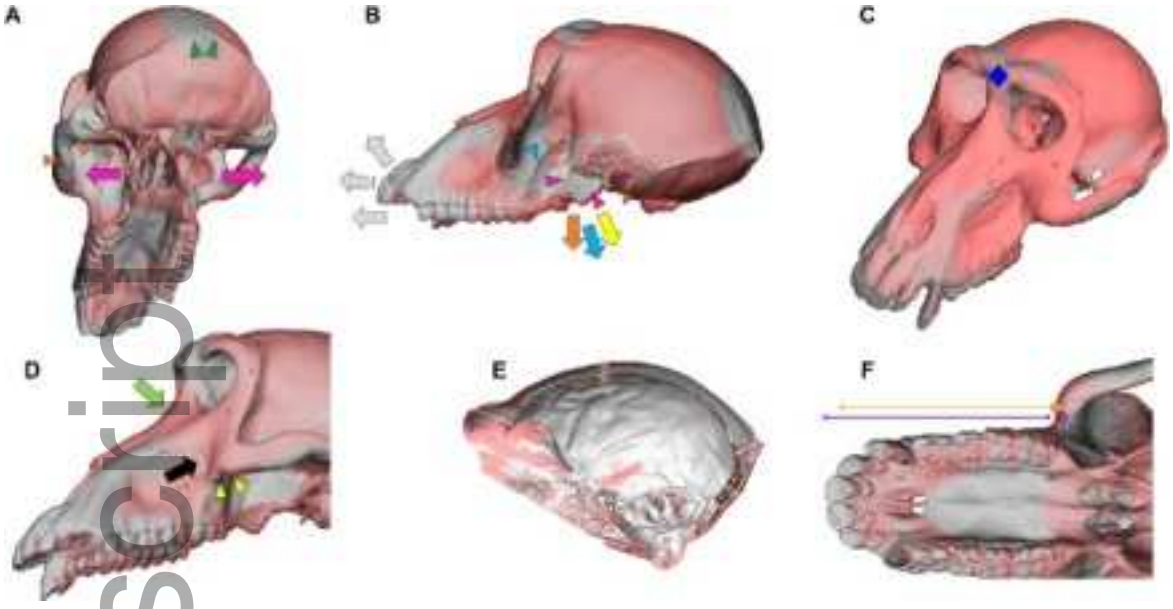

joa_13005_f5.png